Volume 5 Issue 4 (2017) 459-467 ISSN 2347 - 3258
International Journal of Advance Research and Innovation

Laser Direct Metal Deposition (LDMD) – An Overview

Vaibhav Verma [1], Adhirath Mandal [2], Ashish Shukla [3]
[1]TATA Consultancy Services, Bangalore, India
[2]Department of Mechanical Engineering, DTC Greater Noida, India
[3]Department of Mechanical Engineering, Delhi Technological University, Delhi, India

Article Info
Article history:
Received 25 January 2017
Received in revised form
20 June 2017
Accepted 28 July 2017
Available online 15 December 2017

Keywords: LDMD, COMSOL, ANSYS, ABAQUS, Superalloys, Titanium, Manufacturing, Additive Manufacturing, Rapid Prototyping

Abstract
Laser Direct Metal deposition (LDMD) is an additive manufacturing process, it is used to manufacture complex 3D objects directly from CAD files. Laser creates melt region on surface of substrate and powder material blown on to the laser-induced melt pool to form a layer. After a layer deposition, nozzle and laser assembly raised vertically upward by calculated small increment. Next layer is built on previous one, thus a 3D part is built layer by layer. Different FEA Tools were used like COMSOL, ANSYS, ABAQUS etc, and finite element models are developed to numerically simulate heat transfer and coupled thermal phenomena to analyze the influence of various parameters on thermal history. Thermal cycles experienced at different locations and thermal gradient at mutually perpendicular directions are studied. Influence of thermal loading on the model's distortion is analyzed.
LDMD process finds potential application in rapid tooling, prototyping, precision repair work, and manufacture of complex, intricate components with varying compositions, work on challenging materials like Titanium alloys, superalloys etc. Applications are repair of moulds, dyes, motor, gear component etc, work on challenging material(Titanium alloys, superalloys), fabrication of dissimilar metals and so on.

1. Introduction

The laser-aided direct metal deposition (DMD) technique, also known as the laser engineered net shaping (LENS), allows one to fabricate bulk materials from CAD data by layered deposition, through a sequence of melting–solidification of powders, projected by a nozzle usually coaxial to a moving laser beam. Because of its unique characteristics, DMD also allows other applications such as surface treatment (cladding) or parts repair. More precisely, during a DMD process, a laser irradiation creates a molten region on the surface of a substrate. A stream of metal powders is fed into the laser-induced melt pool to form a layer and raise the global volume. The next layer is then built on the previous one, resulting in a 3D part (Figure 1).

In Laser Aided Direct Metal Deposition large number of variables are involved, and experimental investigation is expensive and time consuming, also it does not provide flexibility and ease to improve the process by observe and follow the change in process parameters. There are many factors which are responsible for making the monitoring of the process infeasible, measurement of temperature near the focus of the beam is difficult due to localised nature of heating. Hence productive way to obtain all necessary information is by modelling and analysis, there are many finite element analysis tools available to assist in simulation.

2. Analysis of Heat Transfer

Direct Metal Deposition is a process of shock cooling and heating and the distribution and variation of temperature field has important influence on microstructure, quality, formation of cracks etc, Song et al[2] studied the temperature-time history curves, temperature field distribution, cooling rate and the temperature gradient of the laser cladding forming process. Influences of laser power and scanning speed on the temperature gradient and cooling rate of the cladding layers have been studied, which provided explanation of microstructure forming mechanism, cracking sensitivity and parameter selection. At the same time, LCF experiments have been conducted with parameters obtained from the simulation, microstructure of the cladding layers have been analyzed.

Three-dimensional transient temperature fields were studied with finite element methods, the temperature gradient and cooling rate of Laser Cladding Forming were extremely high, reached 105-106 'C /m and 103-104 'C /s, respectively. Laser power and scanning speed have an significant influence on the size of the melting pool, the cooling rate of the solid-liquid interface and the temperature gradient of the cladding layers, therefore laser power should be adjusted with the proceeding of the processing and the scanning speed should not be too large to prevent cracks.

At the bottom of the melting pool, the temperature gradient G is very large and the cooling rate is very small, the temperature gradient perpendicular to axis Z is predominated. From the bottom to the top of the melting pool, the temperature gradient along axis X increases gradually and the component of axis Z decreases gradually. At the top of the top surface, the temperature gradient along the horizontal exceeds that of the perpendicular direction.

- 316L stainless steel powder as cladding material (melting point 1400 C).
- Common carbon steel 45 as substrate.
- Specific heat and thermal conductivity of 316L stainless steel is time dependent
- Figure 2 shows Laser power 800-3000W, scanning speed 50-240mm/min and spot size 4 x 4 mm2 (Laser power, scanning speed and spot size decides temperature field, temperature gradient and cooling rate of melt pool which in turn decides morphology and crack susceptibility).

Figure 3 show Temp of point 1 varied from 20 C to 2107 C, experience thermal cycle of heating cooling. Quick heating leads to high temperature gradient and cooling rate of melt pool.

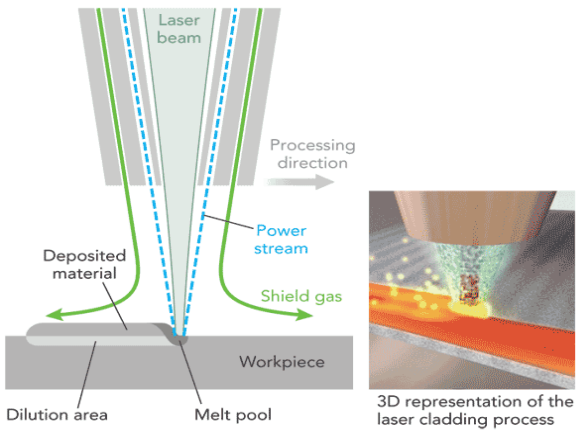

Fig. 1: Schematic of LDMD process[1].

*Corresponding Author,
E-mail: vaibhav.emc2@gmail.com; adhirath.mandal@gmail.com

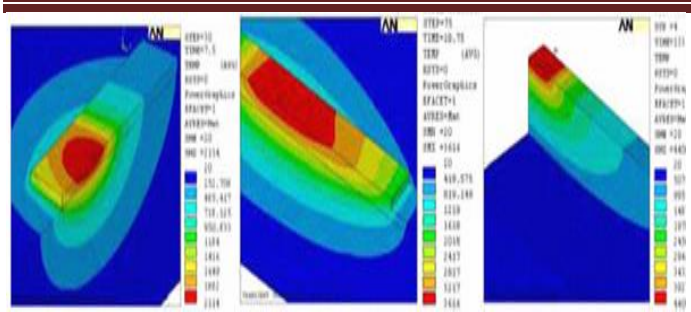

Fig.2: Same power and different time steps, (a) 2000W, 7.5s, (b) 2000W, 18.75s, (c) 2000W, 133.75s [2]

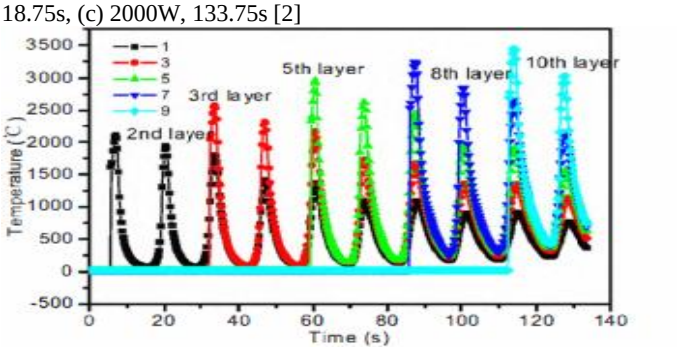

Fig. 3: Temperature time history of mid-section [2]

- High laser power, temperature difference between cladding layer and substrate was smaller.
- In Figure 4 first is for melt pool and second is for solid liquid interface. Cooling rate along solid liquid interface has important influence to microstructure and cracking tendency of cladding layer. High laser power temp difference between cladding layer and substrate was smaller, therefore lower cooling rate.
- As scanning speed increases, highest temperature and gradient decreases, while cooling also decreases. Because too higher scanning speed will result in a poor bonding strength and higher sensitivity of cracking, appropriate scanning speed should be used in order to obtain better forming qualities (Figure 5).
- At bottom of cladding layer, temp gradient along z was biggest and decreases as goes to upper layers. Figure 6
- At upper layers x gradient is more than z.
- heat flow via the substrate is no longer predominating, the heat of the cladding layers radiates through the environment, which can be seen from Figure 6 that at the bottom of the melting pool, temperature gradient along axis Z is predominating while at the top of the melting pool, the gradient along axis X is the maximum.

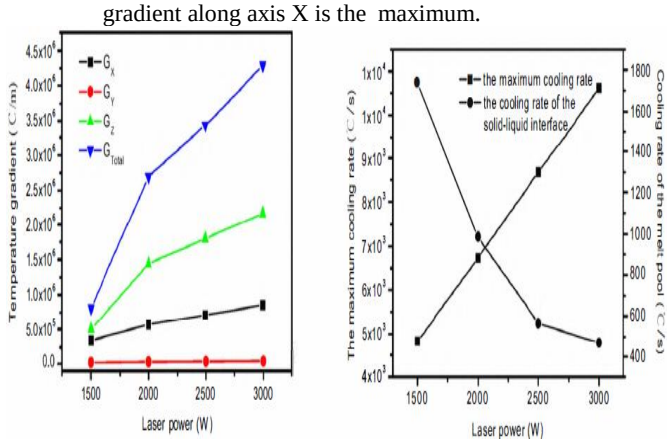

Fig.4: Influence of laser power on temperature gradient and cooling rate [2]

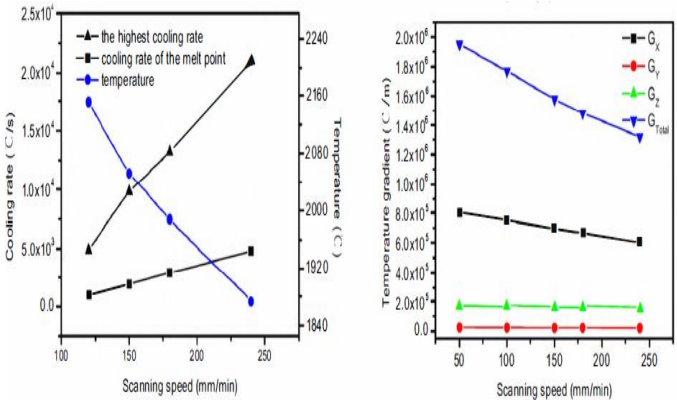

Fig. 5: Influence of scanning speed on temperature gradient and cooling rate [2]

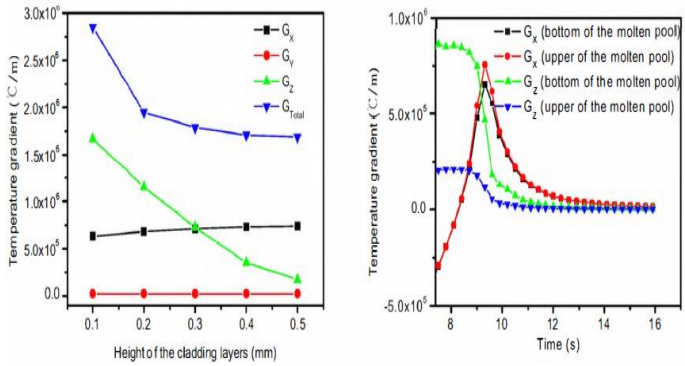

Fig.6 Variation of Temperature gradient with height and time [2]

Peak temperature and thermal cycle experienced by each layer influence the final mechanical properties and dimensional accuracy of the part. An understanding and quantitative knowledge of the peak temperature, melt pool dimensions, and thermal cycles experienced in the deposited layers are essential for a priori selection of the process parameters in LENS technique. Neela et al[3] numerically simulate heat transfer phenomenon in LENS process considering deposition of SS316 powders on a substrate of the same material. The computed temperature profiles are first validated with experimental results reported in the literature. The influence of process parameters on peak temperature, thermal cycle and melt pool dimensions are studied subsequently. The temperature distributions are first computed corresponding to the deposition of a multi-layered thin wall structure (length/width/height ~12:2:6.25mm) into a substrate (length/width/height ~12:6:2 mm) using a laser power and scanning velocity of 275 W and 7.62 mm/s, respectively. Average powder mass flow rate of 3 g/min is considered a layer increment of 250 μm is followed. Figure 7 depicts the computed results of the temperature profile against the corresponding measured results at location 1.6 mm away from the centre of the laser beam along the topmost layer. The horizontal line in Figure 7 indicates the liquidus (melting) temperature of SS316 (1,733 K) and meets both the computed and the corresponding measured temperature profiles at their point of intersection.

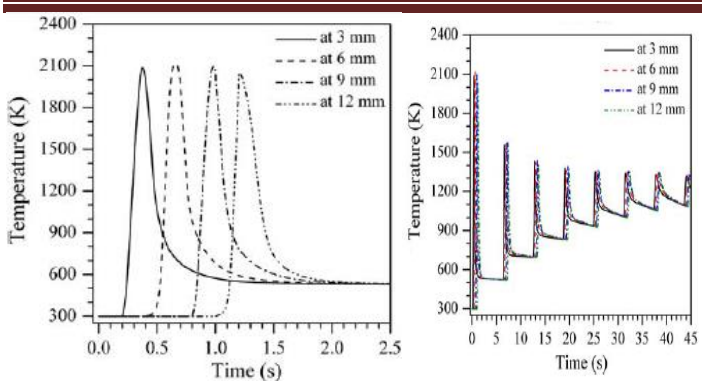

Fig. 7: Variation of temperature along first layer (a) and first eight layers (b) [3]

Figure 7 (a) shows the computed thermal cycles experienced at different linear locations (3, 6, 9, and 12 mm) on the first layer corresponding to a laser power of 400 W, focused beam radius of 1 mm, scanning velocity of 10 mm/s, and a powder mass flow rate of 4 g/min with 60% catchment efficiency. Figure 7 (b) depicts similar computed thermal cycles on the same locations, however, during the building of the first to eighth layers corresponding to the same set of process variables. It is observed in Figure 7 (a) that as the laser beam reaches or is near a particular location, peak temperature shoots to nearly 2,100 K followed by a rapid cooling as the beam moves away. Figure 7 (b) indicates that the peak temperature along the first layer reduces continually as the build height increases and the laser beam also moves up. However, the resident temperature of any layer increases continually. The computed temperature history in Figure 7 (b) conforms to a duration of 1.2 s for the deposition of each layer and an idle time of 5 s between two successive layers, leading to a total time of 44.6 s for completely depositing eight layers.

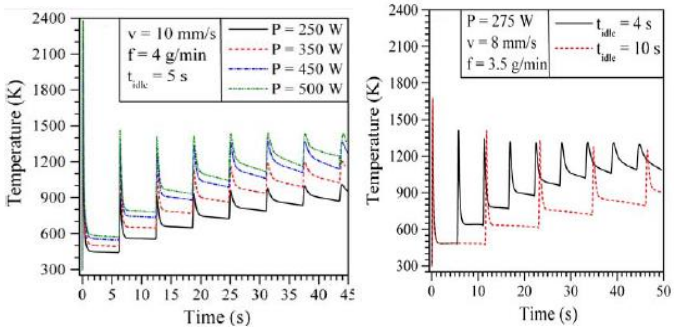

Fig. 8: Variation of temperature with different process parameters [3]

Figure 8 (a), (b) depicts the influence of laser power (P), scanning velocity (v), powder mass flow rate (f), and idle time (t-idle) on the computed values of peak temperature and overall thermal cycle at the initial location on the first layer during the deposition of subsequent layers atop it. Figure 8 (a) shows that both the peak temperature and the resident temperature rise with increasing laser power. This is attributed to the increase in net heat input corresponding to greater laser power. Figure 8 (b) shows that the resident temperature reduces with the increase in the idle time. Jia Yang et al[4] describe the thermal dynamics behaviour in direct laser fabrication (DLF), a model is proposed to be built/ developed based on global model and sub-model pattern. The global model exhibits the heat conduction characteristics of parts in the whole thermal history according to scanning path planning. Contact pairs and gap elements, which consider the effect of the temperature and porosity dependent thermal conduction, are designed in the model to explain powder-to-solid intrinsic transition. The influence of non-linear behaviour of thermal properties in pure nickel on the temperature distribution is estimated as well. Adopting the thermal physical parameters with solid–liquid phase change will make the melted pool temperature higher than that where the solid–liquid phase change parameters are not considered.

It was observed that in the deposition (some point was taken) due to solid-liquid phase change parameters, the melting point temperature attains higher temperature at time 0.72 second. Without influence of solid-liquid phase change parameters the melting point temperature attained at time 0.72 second is lesser. Temperatures on the other locations are higher than the first case however.

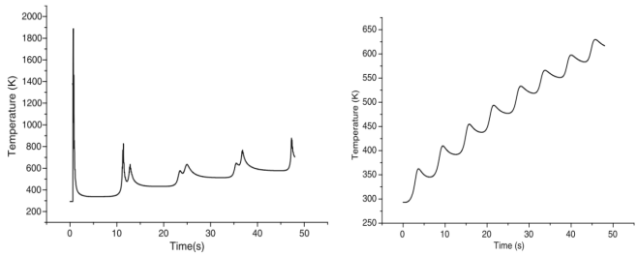

Fig. 9: Thermal history of a point in the substrate (a) and in the deposit (b) [4]

It can be seen that studies of the above mentioned work focus on the thin wall with no more than ten deposited layers. Yongjie Zhang et al[5] built 200 layers of SS410 by LDMD process, (substrate material was set to SS316). Influence of thermal history on microstructure and properties of a multilayer stainless steel (SS410) thin wall built by laser direct metal deposition (LDMD) process was investigated experimentally and numerically by 2 thermocouples. Simulated and measured thermal history indicated that the absorption and loss of heat tended to be close to equilibrium when the deposited material reached a certain height during the LDMD process. Different microstructure regions were formed due to the different thermal history the material experienced. The hardness distribution along the height centerline of the thin wall was measured. The results indicated that thermal history had an important effect on the

Experimental procedure: (Figure 10)

- SS410 deposition on SS316 as substrate (same thermo physical prop but different microstructure)
- Cross sectioned by wire electrode
- Optical microscopy (OM) and scanning electron microscopy (SEM) coupled with an energy-dispersive spectrometer (EDS) were used to investigate the microstructure. X-ray diffraction (XRD) was used for phase identification.

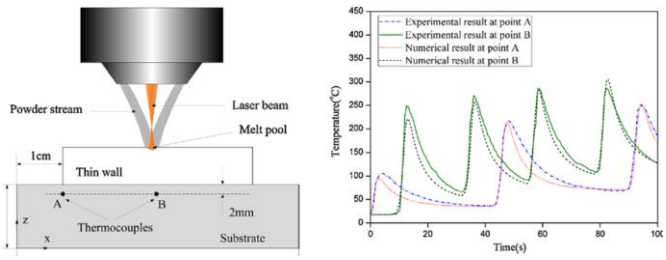

Fig.10: Comparison between simulated and measured values at point A and B [5]

The temperature reached a peak every time the laser beam passed over the measuring point, and then decreased to a resident temperature. Thermal cycle period at point A was the double of that at point B. However, thermal history at the two points had the same changing trend.

Wang et al. (2008)[6] found the similar phenomena and they concluded that the decreasing laser power was required to keep a constant pool size as more layers were deposited.

To make the property analysis from thermal history easier, Zhang Yongjie et al [7] define a critical temperature specific to thermal history and the distribution of it in the part was also discussed. The simulation results indicated that the critical temperature can make the property analysis from thermal history easier. Thermal history of all the deposited materials was similar. It was also concluded that process parameters needed to be time-varying according to the real-time temperature field during the process.

Characteristics of thermal history of points other than mid points are generally not covered and only few layers considered in earlier papers in this paper other points are also being covered and analysis has been done on many layers.

- Thermal history of deposited material at location A, B and C of layers 1, 5 and 10
- Fluctuations tend to dampen as more layers are deposited.
- Peak temperature falls continually
- Resident temperature of cycle increases

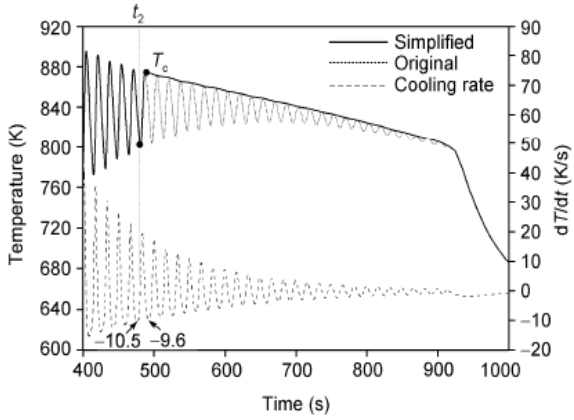

Fig.11: Sketch of the simplification of thermal history[7]

There is also a local minimum of *Tc* at the midpoint of each layer. This is because *a* short time interval of laser irradiations allows less thermal energy to be dissipated. As more layers are deposited, the energy accumulates and the whole temperature of the part increases.

- 10K/s is chosen as critical cooling rate
- Region (t2 till end) can be treated as 1 cycle, peak temp Tc then cools down to room temp.

All the thermal histories of the deposited materials of the part are similar. It can be considered as a sequence of thermal cycles. During the initial stage, the deposited materials experience a significant rapid quenching effect and can attain a very high cooling rate of 103 K/s. Then the peak temperature of thermal cycle decreases and the resident temperature increases continually as the subsequent layer atop it increases. When the deposited materials above reach a certain thickness, the rapid quenching effect decreases and even disappears.

The thermal history of the deposited materials which is dependent on the process parameters has significant influences on the geometric precision and mechanical properties of the final part. Thus better properties can be obtained by maintaining a predetermined steady melt pool temperature field, which requires time-varying process parameters according to the real-time temperature feedback. Atul et al[8] simulated the temperature distribution and single track geometry in Laser Rapid Manufacturing using two dimensional model, and calculated excessive enthalpy above melting point, laser beam size and profile, scan speed, powder feed rate and powder stream diameter with flow distribution is taken from the user. Capability of developed algorithm was developed algorithm was demonstrated by depositing single track on SS316L work piece using Inconel 625 at simulated process parameters. Manavatkar et al[9] Computed values of cooling rate during solidification used to estimate variation in cell spacing of solidified structure. Hall-Petch like relation using cell size as structural parameter is used to estimate hardness distribution. Estimated values of layer-wise cell spacing and hardness remain under predicted and over predicted. Dedrite arm spacing λ used to estimate cooling rate Cr by empirical relation

$$\lambda_2 = A(C_R)^{-n}$$

Where, 'A' and 'n' are material constant.

Grain size is used to measured harness (Hall-Petch)

$$\sigma_y = \sigma_0 + k_y(d_g)^{-0.5}$$

σy and dg refer to yield strength and grain size, σo and Ky refers to lattice resistance and a factor. Attempts are made to numerically predict the influence of process parameters on thermal cycle, residual stress, microstructure, microhardness in deposits of SS304, SS316 and various tool steels.

Hall-petch equation: the equation indicates that strength of metal is equal to frictional stress plus a factor K times the inverse of square root of grain size D. reducing grain size will cause the material to become stronger also increase the toughness.

Cell spacing (or grain size) taken as 3µm, 3D FE model will predict peak temp, melt pool dimension, cooling rate. Cooling rates will be used to estimate layer-wise cell spacing. Cell spacing will be used to estimate microhardness by Hall pech relation. Results are validated with actual multilayer deposit of SS316.

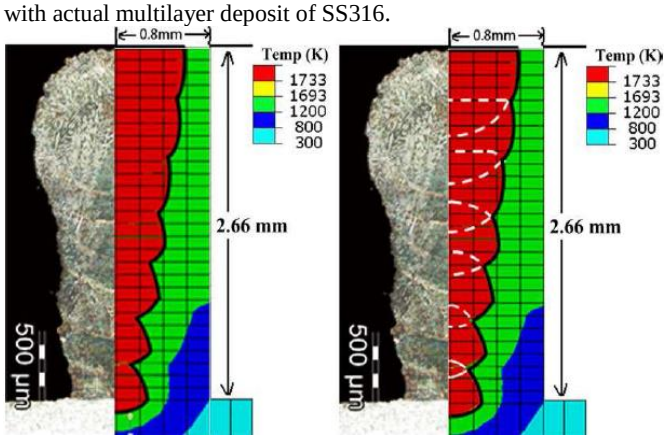

Fig.12: Actual and simulated melt pool profile [9]

- First half of Figure 12 compares actual deposited profile of 7 layers, thick black line is 1733K isotherm.
- Second half of Figure 12 shows simulated melt pool profile.
- White lines also correspond to 1733K isotherm, in dashed since they are inside the pool.
- Reasonable agreement between computed and measured melt pool width and total build height.
- Slight under prediction due to heat transfer to un-melted powder, as broader the 1733K isotherm broader will be the layer thickness.

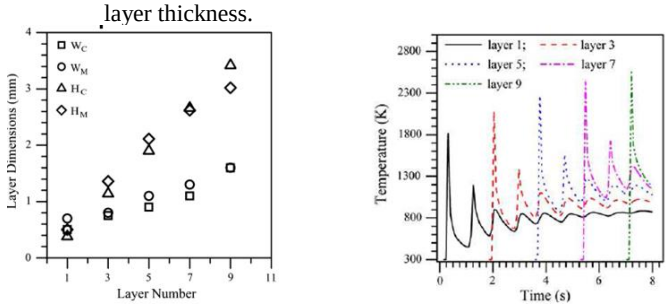

Fig.13: Computed and measured width and height and computed thermal cycles [9]

- Cooling rates reduces with layer deposition.
- High cooling rate in bottom layer due to rapid heat loss through original substrate.

- Cell spacing increase with built height due to decrease in cooling rate.
- Underestimation of cell spacing is due to over prediction of cooling rates.
- Solidification is columnar in all layers.
- Cell orientation follows direction of maximum thermal gradient.
- Hardness decreases with increase in built height.
- Due to reduction in cooling rate and resulting increase in cell spacing.

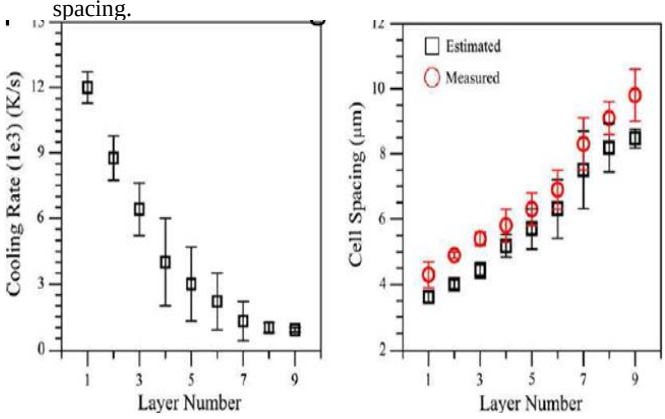

Fig. 14: Computed values of variation in cooling rate and comparison between estimated and measured cell spacing [9]

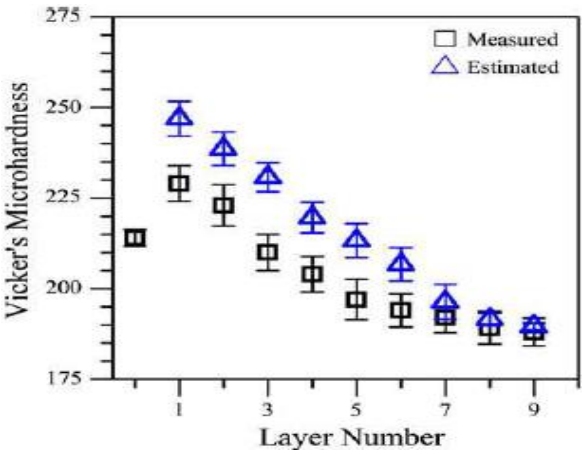

Fig.15: Comparison between estimated and measured micro-hardness in deposited layers [9]

Gangxian Zhu et al[10], discussed the effect of curvature change and accumulation of layers on the temperature field distribution, and was investigated by thin walled rings with different curvatures. it was observed from the numerical results that the temperature of thin wall increases with layer number and its curvature. The rules for changing laser power with layer number and curvature in the processing of thin walled blade can be obtained by simulation when keeping the molten pool temperature stable.

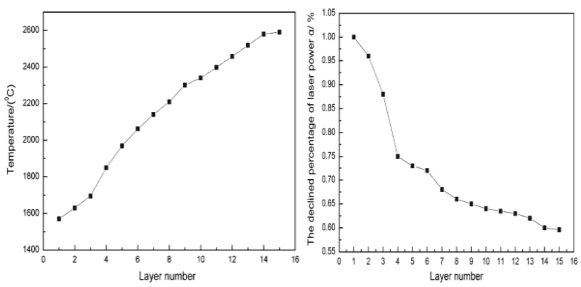

Fig.16: Relation between temperature distribution and the trend of laser power and layer number (a) temperature distribution (b) trend of laser power changing[10]

The model was used to simulate the entire 15-layer LDMD process. Temperature distributions with layer number were shown in Figure 16 (a) above under constant laser power condition. Based on the 1,570°C produced by temperature field computation of the first deposited layer, the trend of laser power changing could be obtained with layer by layer by keeping a constant molten pool temperature, as shown in Figure 16 (b).

It is observed from Figure 16 (a) that the calculated temperature increases with the layer number. Because the substrate is cold during deposition of the first few layers, and as more layers are deposited, they act as a barrier to heat conduction to the substrate, the part becomes hotter and the temperature increases with the layer number. The thin-walled rings with different curvatures can be handled by defining different radiuses. To show influence of different thin-walled rings' radiuses on the molten pool temperature, the molten pool temperature distribution is studied with the radius of R=1, 2, 3, 4, 5, 6, 8, 10, and 15 mm when depositing the first layer. Figures 17 (a) and (b) are showing the typical temperature field distributions of the thin-walled rings with the radius of 1 and 4 mm, respectively.

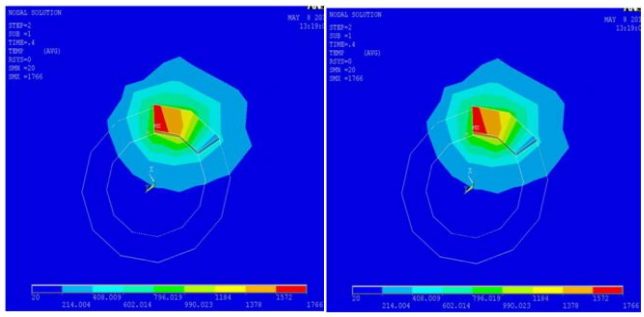

Fig.17: Temperature field distribution with different radius [10]

As can be seen from Figure 18 (a) (keeping power same) the molten pool temperature decreases with the radius, namely, the molten pool temperature increases with the curvature. It is also observed that the molten pool temperature tends to be gentle when the radius is more than 4 mm. This indicates that the influence of the radius on the molten pool temperature is weak when the radius is more than 4 mm. In order to keep the molten pool temperature stable for different radiuses, the trend of laser power changing can be obtained based on the 1,570°C produced by temperature field computation of the thin wall's first layer. And the relationship between laser power and radius was shown in Figure 18 (b) (keeping temperature same).

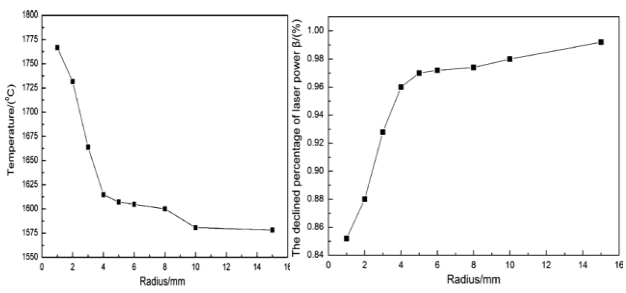

Fig.18: Relationship between temperature distribution and radius [10]

Layer thickness increases gradually with layer number and decreases with radius. Figure 19 (a) with constant laser power, Figure 19 (b) with varied laser power.

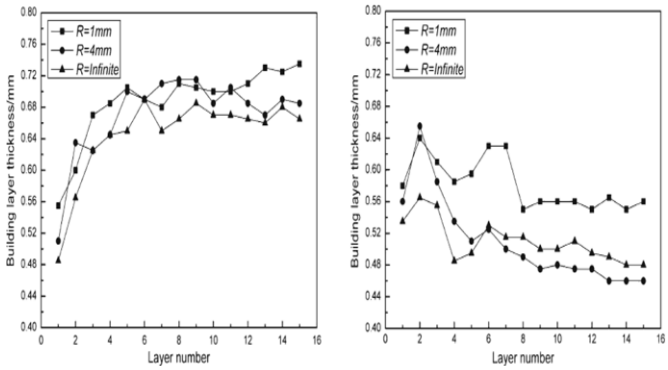

Fig.19: Relation between building thickness and layer number, (a) with constant laser power, (b) with varied laser power [10]

The effects of thin-walled blade's curvature change and accumulating layer number on the temperature field distribution were calculated and the trend of laser power changing with the layer number and curvature in the processing of the thin-walled blade can be obtained by simulation when keeping molten pool temperature stable. The experimental results show that the excessive build-up occurred with constant laser power because of the increase of energy density at corners and the thickness with varied laser power is more uniform than the constant laser power.

3. Analysis of coupled thermal (thermal plus structural)

M. Labudovic et al [11] create a FEM model to calculate transient temperature profiles, dimensions of fusion zone and residual stresses. Model simulations are compared with experimental results acquired on line using an ultra high shutter speed camera which is able to acquire well contrasted images of the molten pool, and off line using metallographic and x-ray diffraction analysis.

As a first step, a high shutter speed imaging is employed in monitoring the deposition of 100 mesh MONEL 400 alloy on AISI 1006 steel, at variety of laser power and scanning speeds. Both numerical and analytic model were developed for thermal history. Results from heat transfer analysis were then used as loads for FE analysis of residual stress and the results were compared with x-ray diffraction technique.

3.1 Assumptions

- Work piece initially at 298K.
- Thermo-physical and mechanical properties are temp dependant.
- Beam diameter at which power density reduced by e^2
- Normal distribution.
- Latent heat of fusion is simulated by artificial increase in liquid specific heat.
- Convective heat flow is neglected.

3.2 Numerical solution to the model

- ANSYS Parametric Design Language to provide heat boundary condition at different time.
- First iteration solve the system equation assuming starting temp 298K.
- Subsequent iteration use temp from previous iteration to calculate conductivity, specific heat matrix.
- First element positioned onto the substrate with set initial boundary condition.
- Subsequent element used results from previous steps as initial condition for each new element birth.
- Iteration continues for time period T until converged solution is achieved or dynamic equilibrium of heat exchange established.
- Study of heat transfer problem allow determination of temp distribution.

3.3 Experiment

- 100 mesh MONEL 400 alloy on AISI 1006 steel, argon was used as shielding gas, Nd-YAG laser
- A fiber optic conducting 337nm wavelength laser
- Nitrogen pulse laser with 5ns pulse duration
- Camera with UV filter thet allow light near 337nm wavelength to pass
- Due to reflection from mirror like molten pool well contrasted image obtained

3.4 Modeling results

- Figure is showing typical analysis from 10mm/s and 600W laser power
- 1325 C isotherm represent fusion zone

3.5 Modeling results (heat transfer analysis)

- Figure 20 shows micrograph of deposits
- a, b shows actual deposit
- c shows numerical modeling
- d shows analytic modeling
- Isotherm corresponding to 1325 C.
- a, b, c, d as obtained by high shutter speed camera, edge detector, numerical and analytic modeling(Edge detection is the name for a set of mathematical methods which aim at identifying points in a digital image at which the image brightness changes sharply or, more formally, has discontinuities. The points at which image brightness changes sharply are typically organized into a set of curved line segments termed edges).
- Pool is deeper at the end than at front due to heat accumulation.
- Increase power and decrease speed widens the pool.

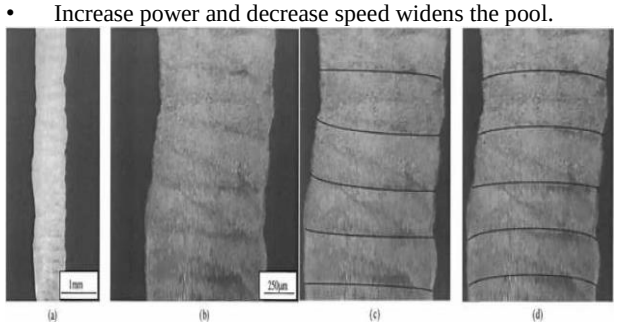

Fig.20: Micrographs of deposits [11]

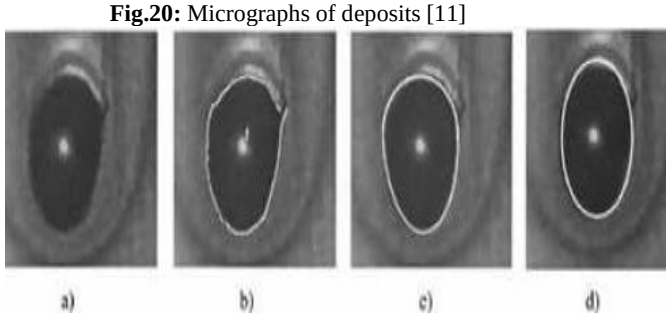

Fig.21: Comparison of melt pool boundaries obtained by the processing result of the edge detector with those obtained by the modelling,(a) original image acquired by high shutter speed camera, (b) processing result of edge detector, (c) numerical modelling result, (d) analytical modelling result [11]

- Isotherm corresponding to 1325 C.
- a, b, c, d as obtained by high shutter speed camera, edge detector, numerical and analytic modeling(Edge detection is the name for a set of mathematical methods which aim at identifying points in a digital image at which the image brightness changes sharply or, more formally, has discontinuities. The points at which image brightness changes sharply are typically organized into a set of curved line segments termed edges).
- Pool is deeper at the end than at front due to heat accumulation.
- Increase power and decrease speed widens the pool.

Stress analysis:

- Sample was allowed to cool down below 50 C between each subsequent build to eliminate preheating effect.
- Residual stress investigated with XRD (Xray diffraction technique is non destructive analytical technique for identification and quantitative determination of various crystalline forms known as phase Identification is achieved by comparing x ray diffraction pattern Study crystal deformation and stress properties)
- Comparison was done with FE modeling.
- Compressive residual stress at the center and tensile towards the edges.
- Effect of subsequent layer is shown in the Figure 22.
- Both figures showing same distribution for 1st layer then progressive increase in tensile residual stress in subsequent layers.
- With layers deposition transverse as well as longitudinal cracks are detected due to stepwise increase in residual stress.
- Cracking can be avoided by preheating, but reduces cooling rate.

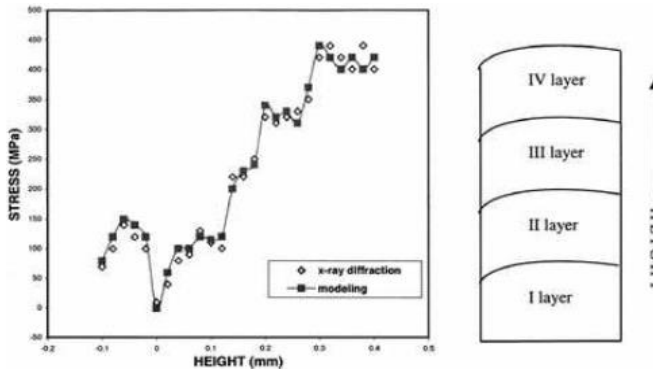

Fig. 22: Distribution of residual stresses within subsequent layer, comparison between x-ray diffraction results and modeling results [11]

- Cracking prevention mechanism by preheating increases ductility of MONEL 400 alloy.
- Preheating treatment to 400C reduces stress to 400MPa.
- Post heating to 600C further reduces stress to 200MPa.
- Simulation gives cross sectional shape of melt pool certified by topside image by camera.
- Modeling of residual stress confirmed by X-ray diffraction residual stress measurement.

A three-step analytical and numerical approach was carried out by Peyre et al [12] to predict the shapes of manufactured structures and thermal loadings induced by the DMD process. First, powder temperature was calculated using a analytical model, then the geometry of walls was predicted by a combined numerical + analytical modelling, finally thermal behaviour during DMD of a titanium alloy was described.

The thermal model takes into account the moving interface during metal deposition with a specific function κ (t, x, y, z) allowing the conductivity front to move simultaneously with the moving laser source (with an appropriate spatial energy distribution), thus representing rather precisely the DMD process. This allowed us to provide an adequate representation of temperatures near the melt-pool, and to reproduce with a good accuracy thermal cycles and melt-pool dimensions during the construction of up to 25-layer walls. This was confirmed by comparisons with experimental thermocouple data $T = f(t)$, and fast camera melt-pool recording.

Following these works, our objective was to propose a combined analytical–numerical approach, to predict geometries and thermal fields involved during a DMD process, considering only the experimental parameters such as mass feed rate Dm (g min−1), laser power (W) and scanning speed V (m s−1) as input data.

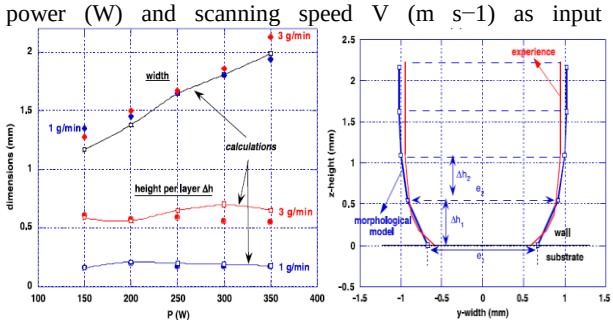

Fig.23: Comparison between experimental data and simulated values, (a) influence of laser power and mass feed rate on the stabilizing geometrical features of a DMD wall [12]

Experimental validation: Dedicated DMD experiments were carried out (between 1 and 8 layer), using different parameters (mass feed rate in the 1–4 g min−1 regime, laser powers between 100 and 400 W), to compare with simulations results. The global agreement between experimental data and calculations is satisfactory Figure 23. Calculated widths and average deposition heights are well reproduced (15% maximum difference) by measurements carried out on cross-sections, over a rather wide range of laser and powder feeding conditions. Moreover, the simulation-aided morphological model allows describing with a reasonable agreement the evolution of geometrical parameters with the number of layers n as shown in Figure 23. Consequently, the theoretical approach seems to be accurate enough to predict the geometry of walls before performing finite element thermal simulations.

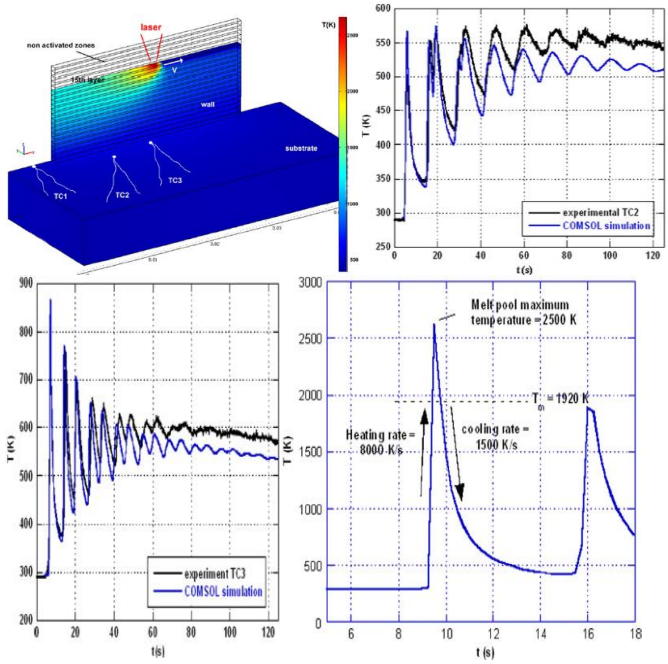

Fig.24: Comparison between experimental and simulated profiles (600 W, 0.006m/s), (a) thermocouple TC2, (b) TC3 (c) Temperature versus time simulated in the middle of the wall [12]

Experimental $T = f(t)$ profiles exhibit a quasi-sinusoidal aspect corresponding to the alternated displacement of the laser head Figure 24. With a 35% absorptive of the laser beam, it appears that COMSOL simulations allow one to reproduce rather well those temperature-time profiles recorded by thermocouples, whatever the process parameters. Thermocouple data obtained with 5 or 6 thermocouples located at various positions in the substrate, and near the wall, are systematically well reproduced. This is particularly true concerning the global thermal chronology, but also for the first $T = f(t)$ peak corresponding to the first layer, and for all the following

peaks corresponding to the 2nd , 3rd . . . layers Figures 24(*a*) and (*b*). This has been confirmed for various mass feed rates *D*m (g min−1), various scanning speeds *V* (m s−1) and various laser powers *P* (W), for a unique 0.35 absorptive value.

We can also obtain local temperature versus time data into the wall Figure 24 (c), and deduce numerically heating and cooling rates, together with the tempering temperature which corresponds to the average temperature achieved in the wall after a long manufacturing time.

Melt-pool sizes (length and height) are slightly overestimated by simulations. The melt-pool enlargement is due to lower heat dissipation far from the substrate and contributes to wider walls until the melt pool reaches a stabilized value

This DMD global model has already been successfully applied and validated on other aeronautical alloys such as Inconel 718 or Rene 142.

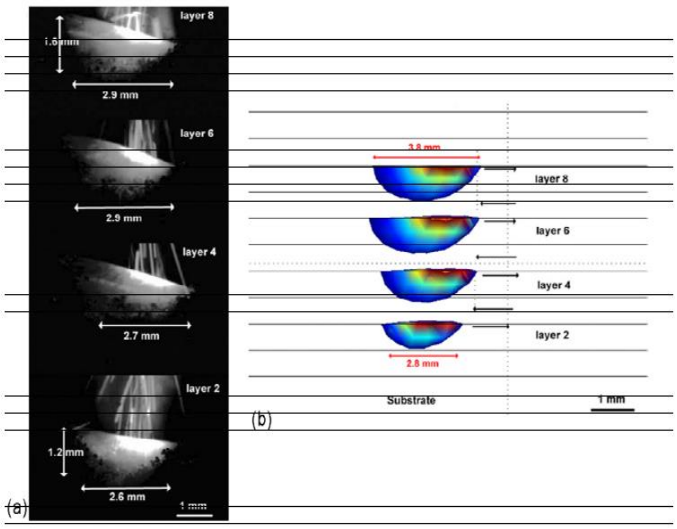

Fig. 25 : Comparison between (a) experimental (1000 Hz C-Mos fast camera), (b) simulated laser induced melt pool (600W, 0.006 m/s), between 2nd and 8th manufactured layers [12]

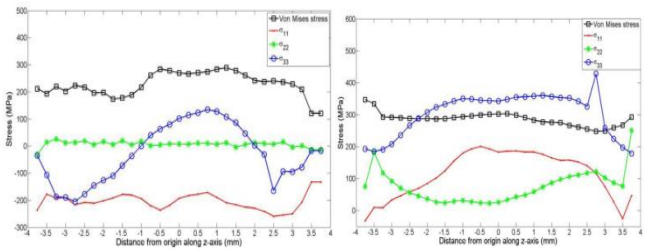

Fig.26: Residual stress on (a) top surface, (b) bottom surface of deposit along z direction [13]

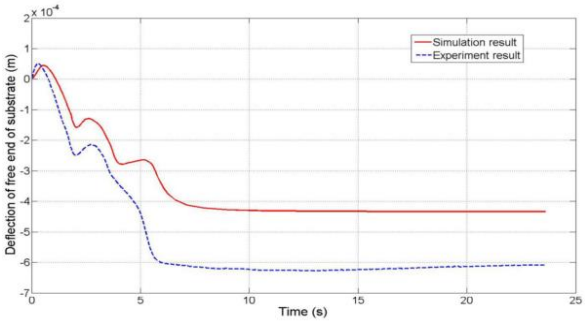

Fig.27: Simulation and experimental results of deflection of substrate [13]

The process of DMD involves very high thermal gradients and heating and cooling rates, resulting in residual stresses and distortion, Heng Liu et al [13] presented a thermo-mechanical finite element model to predict residual stress and deformations. The thermal distribution, thermal stress field, geometry deformation and effect of deposition parameters on residual stress and deflections are explained.

Normal and Von-Mises stress at top and bottom are shown in Figure 26 (a) and (b).

Unlike most of the analysis the workpiece is fixed from the left side and deposition is added up at the centre area.

In the plot of Figure 27 the trend of deflection first bend down due to thermal expansion on the top surface and then bend up during the cooling process, after completely cool down substrate keeps the deformed shape.

Verma and Shukla presented LMD thermal analysis using Ansys Parametric Design Language (APDL) based FEM to simulate a moving heat source for SS316 and Ni [14]. The overall conclusions derived from an in-depth literature review are listed in [15].

Shukla and Verma modelled different cases and numerically analysed the LDMD process[16].

4. Conclusions

1. As the layers increases cooling rate decreases towards the top layers.
2. At the bottom of the molten pool temperature gradient is high and cooling rate is small.
3. From bottom to the top of the melting pool, temperature gradient along X axis (horizontal axis) increases gradually and the component of Z axis (vertical axis) decrease gradually. As the layers increases the thermal gradient along the horizontal exceeds that of the vertical direction.
4. The peak temperature experienced by a particular layer gradually reduces as the laser beam moves to the higher layer.
5. Deposited layers undergo high cooling rate which is particularly at its highest at the solid-liquid interface and decreasing with the increasing distance from the centre of the melt pool.
6. With the increase in build height, the heat loss towards the substrate is reduced, and thus, heat input per unit length needs to be reduced to avoid over-melting along the top layers.
7. Laser power, scanning velocity, powder mass flow rate, and idle time between the deposits of successive layers influence the thermal behavior induced in the deposited material.
8. Thermal history of the deposited material at different locations has the same changing trend.
9. During the initial stage, the deposited material experience a quenching effect and can attain a very high cooling rate. Then the peak temperature of thermal cycle decreases and even disappear and the resident temperature increases continually as the subsequent layer atop it increases.
10. For constant laser power and scanning speed, the layer width and peak temperature increases while the cooling rate decreases towards the top layers.
11. Solidified deposit has cellular structure with increase in cell spacing as the cooling rate reduces towards the top layers.
12. Too higher scanning speed will result in a poor bonding strength and higher sensitivity of cracking, appropriate scanning speed should be used in order to obtain better forming qualities.
13. Excessive build up occurred with constant laser power because of the increase of energy density at corners and high curvatures and thickness with varied laser power (keeping temperature same) is more uniform than constant laser power.

14. Molten pool developed during the process is deeper at the end than at the beginning because of the heat accumulation.
15. In comparison with single layer, subsequent layer built result in an increase in residual stresses.
16. Cracking may occur laterally or longitudinally. Cracking can be avoided by preheating the specimen.

Reference

[1] http://www.industrial-lasers.com/articles/print/volume-250/issue-6/features/laser-metal-deposition.html
[2] S Jianli, L Zhiqi, Q Huiping, DU Shiwen, LI Yongtang, D Qilin.Numerical simulation of the three-dimensional temperature field in Laser cladding forming process, 2008
[3]V Neela, A De. Three-dimensional heat transfer analysis of LENS process using finite element method, International Journal on Advanced Manufacturing Technology, 45, 2009, 935–943
[4] J Yang, F Wang. 3D finite element temperature field modelling for direst laser fabrication, International Journal on Advanced Manufacturing Technology, 43, 2008, 1060-1068
[5]Y Zhang, G Yu, X He, W Ning, C Zheng. Numerical and experimental investigation of multilayer SS410 thin wall built by laser direct metal deposition.
[6] L Wang, S Felicelli, Y Gooroochurn, PT Wang, MF Horstemeyer. Optimisation of the LENS process for steady molten pool size. Mater. Sci. Eng. , 2008,148-156
[7] Z YongJie, YU Gang, HE XiuLi, Numerical study of thermal history in laser aided direct metal deposition process, 2012
[8] A Kumar, CP Paul, AK Pathak, P Bhargava, LM Kukreja. A finer modeling approach for numerically predicting single track geometry in two dimensions during Laser Rapid Manufacturing, Optics and Laser technology 44, 2012, 555-565
[9] VD Manavatkar, AA Gokhale, GJ Reddy, A Venkataramana, A De. Estimation of melt pool dimensions, thermal cycle, and hardness distribution in the Laser Engineered Net Shaping process of austenitic stainless steel, The minerals, metals and materials society and ASM international, 2011.
[10] G Zhu, A Zhang, D Li, Y Tang, Z Tong, Q Lu. Numerical simulation of thermal behaviour during laser direct metal deposition International Journal on Advanced Manufacturing Technology 55, 2011, 945-954
[11]M Labudovic, D Hu, R Kovacevic. A 3D model for direct laser metal powder deposition and rapid prototyping. Journal of Material science, 38(1), 2003, 35-49
[12]P Peyre, P Aubry, R Fabbro, R Neveu, A Longuet. Analytical and numerical modelling of the direct metal deposition laser process, Journal Physics D: Applied Physics 41, 2008, 10
[13] H Liu, TE Sparks, FW Liou, DM Dietrich. Numerical Analysis of thermal stress and deformation in Multi-Layer Laser Metal Deposition Process, 2013
[14] V Verma, M Shukla. Laser metal deposition thermal analysis using finite element method, Proceedings of the 15th International RAPDASA conference, Stellenbosch, South Africa, November 2014.
[15] V Verma, Finite Element Analysis of Laser Metal Deposition, M.Tech. Thesis (unpublished), Mechanical Engineering Department, MNNIT Allahabad, India, 2014.
[16] M Shukla, Vverma. Finite Element Simulation and Analysis of Laser Metal Deposition, 6th International Conference on Mechanical, Production and Automobile Engineering (ICMPAE'2014) Cape Town, South Africa, Nov. 27-28, 2014